

Original Article | ISSN (0): 2582-631X

DOI: 10.47857/irjms.2025.v06i04.07132

Performance Enhancement of Modified DSOGI-PLL for Power **Quality Improvement in Grid-Connected PMSG System**

 $Devang \ B \ Parmar^{1*}, A shutosh \ K \ Giri^2$ 1 Gujarat Technological University, Ahmedabad, Gujarat, India, 2 Government Engineering College, Bharuch, Gujarat, India. *Corresponding Author's Email: devang.parmar.el@vvpedulink.ac.in

Abstract

This study investigates the efficient operation and advanced control of a wind energy conversion system (WECS) incorporating a grid-connected permanent magnet synchronous generator (PMSG). The proposed methodology employs a generator-side vector control strategy integrated with a modified flux-weakening current controller, enabling precise rotor speed tracking and accurate angle estimation through a reference dq-axis current control loop. This design ensures optimal energy capture, smooth system operation, and enhanced transient performance under variable wind conditions. Although the conventional Dual Second Order Generalized Integrator Phase-Locked Loop (DSOGI-PLL) performs satisfactorily under ideal grid conditions, its synchronization, accuracy and responsiveness degrade during disturbances such as harmonics and frequency fluctuations. To overcome these limitations, a Modified Quasi-Type-1 DSOGI-PLL is introduced, incorporating adaptive gain tuning and improved harmonic suppression to provide robust phase tracking and fast dynamic adaptation. This enhanced PLL is embedded within the overall PMSG control framework, with an emphasis on DC-link voltage stabilization and maintaining power quality at the point of common coupling (PCC). Extensive MATLAB/Simulink-based simulations under disturbed grid scenarios validate the proposed approach, demonstrating improved synchronization dynamics, reduced total harmonic distortion (THD), and superior voltage regulation, and greater operational robustness, thereby supporting reliable and grid-compliant renewable energy integration.

Keywords: Dual Second Order Generalized Integrator (DSOGI), Grid Synchronization, Phase-Locked Loop (PLL), Power Quality, Wind Energy Conversion System (WECS).

Introduction

Advanced control mechanisms for grid-connected power converters in renewable energy systems, storage systems, and electric vehicles were reported in earlier studies, where researchers emphasized their role in supporting the energy transition and enhancing grid reliability (1). It was stated in past research that the review begins with WECS, where key components such as wind turbine generators (WTGs), power electronic converters (PECs), and grid integration challenges were highlighted (2). Advanced control strategies for both generator and grid side converters were discussed in past research to improve system performance and stability. Key technical issues, including generation uncertainty, power quality, voltage stability, reactive power support, and fault tolerance, have been reviewed along with mitigation strategies, such as energy storage systems, grid codes, and policy frameworks, which are essential for sustainable integration. Grid-side issues such as fault ride-through (FRT), harmonics,

and flicker have been addressed in previous studies. A comprehensive overview of WECS modeling, control, and integration challenges associated with wind intermittency has been presented in past studies (3). Generator-side control ensures precise torque and current regulation, whereas grid-side control enhances power quality and DC-link stability. A variablespeed PMSG-based WECS employing vector control for optimal power extraction and seamless grid integration was reported in earlier research (4). It was reported in past research that torque was controlled on the machine side through the stator current in the DQ frame, whereas the gridside control was implemented using an SSLKF algorithm for reference current generation, power quality enhancement, and DC-link regulation (5). The reliability and efficiency of grid-connected PMSG-based wind systems using a back-to-back converter with a common DC link have been analyzed in past studies (6). In previous research,

This is an Open Access article distributed under the terms of the Creative Commons Attribution CC BY license (http://creativecommons.org/licenses/by/4.0/), which permits unrestricted reuse, distribution, and reproduction in any medium, provided the original work is properly cited.

(Received 23rd July 2025; Accepted 08th October 2025; Published 30th October 2025)

a data-driven robust control strategy for machineside and M3C grid-side converters was developed to enable grid-forming control in low-frequency wind turbines, with real-time simulations confirming the effectiveness of the controller (7). A predictive-backstopping control strategy has been proposed to improve the dynamic performance of grid-connected PMSG-based wind systems, which demonstrated reduced ripples, faster responses, and lower computational loads (8). The type-3 MNF-SOGI-PLL effectively eliminated phase errors caused by DC offsets and scaling disturbances without compromising dynamic performance, offering fast response, improved grid parameter estimation, and enhanced stability. A PLL is a nonlinear negative-feedback control system that aligns its output frequency and phase with those of the input signal. PLLs are widely applied in power electronics for synchronizing grid-connected converters, as well as in various control and monitoring applications (9).

Recent studies have provided a comprehensive overview of the advancements in PLL design for three-phase systems. An improved PLL parameter design has been proposed to mitigate the coupling effects in the control loop, thereby enhancing the system stability and robustness against grid impedance variations (10). An adaptive control strategy for a three-phase induction generator was developed to improve power quality under varying load and grid conditions, with optimized PI gains ensuring dynamic stability and reduced harmonics (11). In past work, a robust standalone DG system integrating wind, PV, and battery storage was presented, controlled by an ANLMAT-based adaptive algorithm, achieving a THD of 3.29% under dynamic and unbalanced conditions (12). Earlier research proposed a synchronization and control strategy for a standalone DG system using an improved complex coefficient filter-based PLL (ICCF-PLL), which ensured a fast dynamic response, enhanced power quality, voltage/frequency stability (13). A novel SSLKF-FLL-based control algorithm was proposed by researchers to enhance power quality and dynamic response over traditional PLL and SRF methods, with PI gains optimally tuned using the Crayfish Optimization Algorithm (14).

Further, design-oriented studies on advanced PLLs, such as DSOGI-PLLs, multiple reference frames, and complex coefficient filter-based PLLs

were proposed in prior studies to improve smallsignal modeling and stability analysis. The Enhanced PLL (EPLL) method has been proposed to improve the robustness and transient response under voltage unbalance and harmonic distortion (15). High-speed synchronization methods were introduced in earlier studies for symmetrical component extraction which are useful for protection and control in unbalanced grid environments, along with modeling and design guidelines to improve stability and robustness under grid variations (16). Multiple reference frame-based control strategies were proposed in previous research to enhance performance under distorted and unbalanced input conditions (17). Novel control strategies combining FFOC and DPC were proposed in earlier studies to improve power regulation and dynamic response for PMSG-based wind turbines to improve power regulation and dynamic response (18). It was found in past research that the DDSRF-PLL achieves superior harmonic rejection and fast synchronization for grid-connected converters (19). Frequency stability in VSG-controlled PMSG systems has been explored to enhance the virtual inertia emulation under high renewable penetration (20). Optimal transient control schemes were proposed in earlier studies to ensure stable operation during faults and grid transitions (21). A simple method for rejecting the DC offset in single-phase SRF-PLL systems has been proposed to improve phase detection accuracy and steady-state response (22). A Modified Quasi-Type-1 DSOGI-PLL was designed in recent research to overcome the shortcomings of conventional and advanced PLL techniques. Unlike the traditional DSOGI-PLL, whose synchronization accuracy degrades under harmonics and frequency deviations, the proposed structure incorporates adaptive gain tuning and enhanced harmonic suppression, thereby ensuring a faster dynamic response and robust operation (23). Compared with improved PLL and decoupled PLL approaches reported in past research, the proposed significantly reduces design computational complexity by avoiding multiple transformation stages, making it well suited for real-time digital implementation (24).Furthermore, unlike adaptive notch filter PLLs, which provide strong harmonic rejection at the expense of slower dynamics, the proposed method achieves both high harmonic immunity and fast

synchronization. These advantages highlight the novelty and practical relevance of the proposed PLL framework in enhancing the power quality and ensuring reliable grid integration of PMSG-based wind energy systems (25). Popular control applications in wind energy conversion systems based on PMSGs have been reviewed, and their efficiency and adaptability were emphasized (26). Various wind generator systems have been comprehensively compared, and their operational differences and performance characteristics were highlighted (27). Small-signal stability of PMSG, DFIG, and SCIG-based wind farms has been analyzed to evaluate their dynamic responses under grid disturbances (28). The least-

logarithmic mean filter (LLMF) control algorithm was implemented in grid-tied SPV-DSTATCOM systems, and improved harmonic mitigation and reactive power compensation were demonstrated (29).

Comparative Analysis of PLL Methods

A comparative analysis is presented between the proposed Modified Quasi-Type-1 DSOGI-PLL, the conventional DSOGI-PLL, and other advanced PLL methods. The comparison focuses on the structural complexity, frequency adaptability, harmonic rejection capability, dynamic response, and real-time implementation feasibility. The consolidated summary is presented in Table 1.

Table 1: Comparative Analysis of Different PLL (9)

PLL Method	Structure	Frequency	Harmonic	Dynamic
FLL Methou	Complexity	Adaptability	Rejection	Response
Traditional DSOGI-PLL	Low	Limited	Moderate	Moderate
Improved PLL	Moderate	Better than DSOGI-PLL	Good	Good
Adaptive Notch Filter PLL	Moderate-High	Wide frequency range	Very good	Slower (due to adaptation)
Decoupled dq-PLL	High	Good for unbalanced grid	Good	Good
Proposed Modified Quasi-Type-1 DSOGI-PLL	Moderate	Wide frequency range	Excellent	Fast and Stable

Literature Gap and Motivation

- Although conventional DSOGI-PLL structures have been widely adopted for synchronization in grid-connected converters, several limitations persist. Prior studies have reported a slow dynamic response, degraded accuracy under harmonic distortion, and high sensitivity to grid variations.
- These shortcomings hinder reliable operation, particularly under weak or distorted grid conditions, which are increasingly common in modern renewable energy systems. To address these gaps, the present study proposes a Modified Quasi-Type-1 DSOGI-PLL that incorporates adaptive gain tuning and enhanced harmonic suppression. These modifications ensure faster synchronization, reduced estimation error, and robust performance under non-ideal grid conditions.
- The practical feasibility and industry relevance are demonstrated as the proposed method requires minimal computation, no additional hardware, and full compatibility with low-cost

- DSP/FPGA platforms. Its modular design allows seamless integration into existing converter control frameworks, while compliance with IEEE 519 limits ensures improved power quality, reduced penalties, and greater system reliability under weak grid conditions, all without significant added cost. The highlighted bullet points describe the author's contribution.
- The development of a generator-side vector control strategy integrated with a modified flux-weakening current controller ensures precise rotor speed tracking and smooth operation across variable wind speeds.
- The development of a Modified Quasi-Type-1
 DSOGI-PLL with adaptive gain tuning and
 harmonic suppression to improve
 synchronization accuracy and dynamic
 response under distorted grid conditions.
- Performance improvements were validated through MATLAB/Simulink simulations, showing reduced settling time, improved phase

tracking, and a frequency estimation error below 0.1 Hz.

 Enhanced power quality and grid compliance, achieving DC-link voltage stability within a nominal value of ±5 V, and reducing the injected current THD to 2.23%, meeting IEEE 519 standards.

Methodology

System Model and Description

The proposed WECS utilizes a PMSG directly coupled to a wind turbine to convert mechanical energy into electrical energy efficiently. The generator-side converter is governed by a hysteresis PWM scheme and supported by a flux-weakening controller, which enables extended

speed operation beyond the rated wind speed. The system configuration employs Maximum Power Point Tracking (MPPT) to derive the reference power based on wind conditions, which is then converted into torque and current references using a PI controller and d-q transformations. These references guide the generator-side converter to maintain optimal power generation. The DC-link capacitor stabilizes the intermediate voltage, serving as an energy buffer between the generator and grid-side converters. The grid-side converter, also controlled via hysteresis PWM, regulates the current injection into the grid while compensating for nonlinear loads that introduce harmonic distortions (26). Figure 1 shows the detailed control diagram.

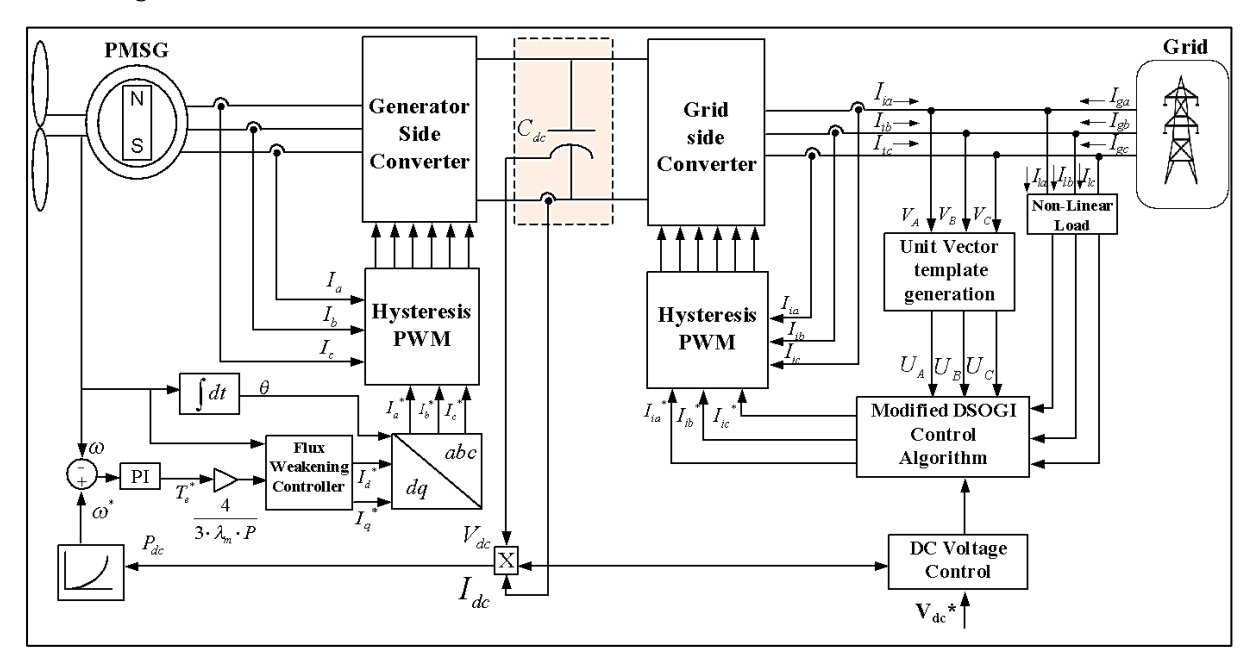


Figure 1: Control Strategies for a Grid-Connected Wind-Integrated PMSG System

To ensure clean power delivery, the system incorporates a modified dual second-order generalized integrator (DSOGI) control algorithm (23). This algorithm processes distorted grid voltages and generated unit vector reference signals to extract the fundamental frequency components. These are used to generate accurate reference currents, thereby maintaining sinusoidal grid injections. A unit vector template generation module ensures phase synchronization under voltage imbalances and distortions. Meanwhile, a DC voltage controller maintains the DC-link voltage at its reference value and coordinates with the DSOGI to support dynamic power regulation.

This integrated control scheme ensures high power quality, harmonic mitigation, and stable operation of the PMSG-based WECS under fluctuating wind conditions and varying nonlinear loads.

Generator-Side Closed-Loop Vector Control

The power equation and fundamental operational principle of wind turbines, which govern aerodynamic energy extraction, are outlined below. The power equation and fundamental principle of wind turbines are as follows:

$$P = \frac{1}{2} \rho C_p A V^3$$

$$T_{turbine} = \frac{1}{2} \rho A C_p \frac{V}{\gamma}$$
[2]

The energy output of wind turbines is affected by the turbine design, wind speed, and prevailing weather conditions. Wind turbines operate optimally within a specific wind speed range and may cease operation or adjust their blade pitch to mitigate damage from high-velocity winds. Wind turbines typically aggregate on wind farms to enhance their power-generation capacity. The cumulative turbine output of a wind farm constitutes power production (27). Table 2 shows the influence of wind speed on various parameters associated with the wind characteristics.

Table 2: Impact of Wind speed on Different Parameters

Wind Velocity (p.u)	Wind Speed (m/s)	MPPT Power (p.u.)	MPPT Power (Watt)	Generator Speed (p.u.)	Generator Speed (rad/sec)	Mechanical Torque (Nm)
1.04	13	0.7019	2597	1.2	95.83	-43.10
0.96	12	0.5886	2178	1.105	88.26	-36.81
0.88	11	0.4564	1688	1.065	85.02	-28.74
0.8	10	0.3563	1323	0.9879	78.92	-22.90
0.72	9	0.2788	1031	0.899	71.86	-18.16
0.64	8	0.206	762	0.8062	64.39	-14.10
0.56	7	0.1413	522.8	0.7056	56.36	-10.79

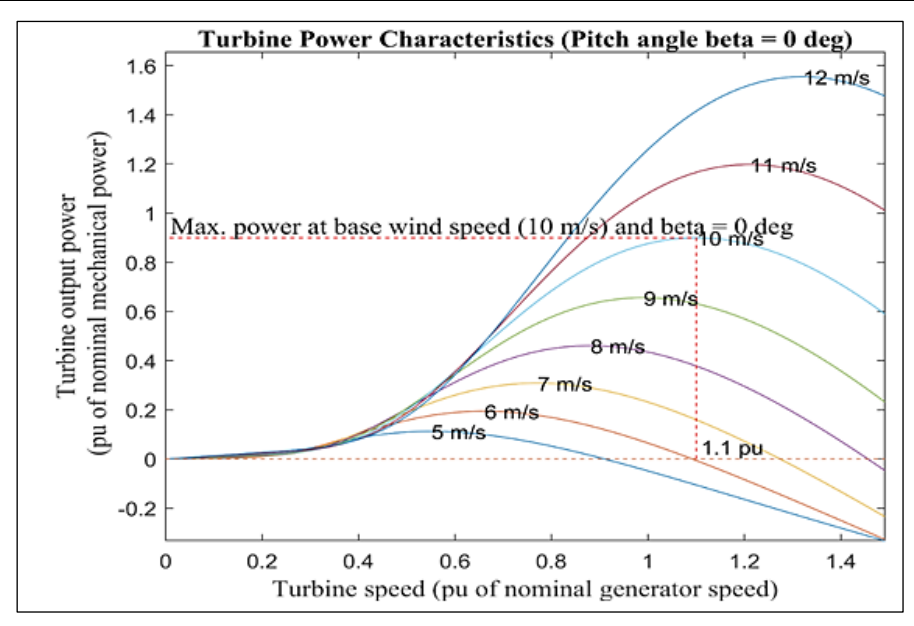


Figure 2: Power–Speed Characteristics of the Wind Turbine

The power–speed characteristics of the wind turbine are shown in Figure 2. The wind speed fluctuated between 10 m/s and 12 m/s. In the 8-pole PMSG control design, the generator rotational speed was 750 rpm, with an average wind speed of 10 m/s. The generator reached a maximum power output of 1.2 p.u. decreasing to 0.7 p.u. below this speed. Figure 3 shows the turbine power profile. The PMSG 3.7 kW wind turbine achieves peak

power output at 0.9 p.u. maintaining this power until the wind speed reaches 10 m/s. To demonstrate the wind turbine power characteristics, the rotational speed was adjusted to 1.1 times the base generator speed. Pitch angle beta remained constant at zero. To represent the PMSG dynamic prototype in a rotating reference frame, the mathematical modelling formulas below were used:

$$\begin{split} V_{q} &= L_{q} \, \frac{di_{q}}{dt} + R_{s} \, i_{q} - w_{r} \, \lambda_{m} + w_{r} \, L_{d} \, i_{d} \\ V_{d} &= R_{s} i_{d} + L_{d} + \frac{di_{d}}{dx} - w_{r} L_{q} i_{q} \end{split} \tag{3}$$

To express the electromagnetic torque produced by the rotor, the following equation can be used:

$$T_{e} = \left(\frac{3}{2}\right) \left(\frac{P}{2}\right) \left[\left(L_{d} - L_{q}\right) i_{q} i_{d} - \lambda_{m} i_{q}\right]$$
[5]

When a cylindrical rotor is utilized, both L_d and L_q are reduced, thereby transforming the equation into a suitable representation.

$$T_e = \left(\frac{3}{2}\right) \left(\frac{P}{2}\right) \lambda_m i_q$$

The significance of the quadrature axis reference-current element can be estimated using the following formula:

$$i_q^* = \frac{4}{3} \left(\frac{T_e^*}{P \, \lambda_m} \right) \tag{7}$$

The equations above delineate the interaction between the electrical and mechanical components of a PMSG when it is represented in a reference frame that is in motion. To model and study the behaviours of the PMSG and integrate these equations over time, considering the starting conditions and external factors, such as load torque or wind speed, control methods can be used to change how the generator works to meet certain requirements, such as keeping the amount of electrical power produced steady or controlling the speed of the wind machine.

Figure 3 illustrates the MATLAB Simulink-based control logic for flux weakening, enabling extended

speed operation of the PMSG through the dynamic adjustment of the d-axis current. The flux-weakening control strategy of the PMSG, based on lookup tables, is shown in the control logic diagram below. The system adjusts the i_d^* and i_q^* reference currents based on the rotor speed and torque command, particularly when the speed exceeds the base speed. Table 3 presents the flux-weakening logic along with its corresponding mathematical representation, outlining the relationship between the rotor speed and d-axis current for effective high-speed control of the PMSG (28).

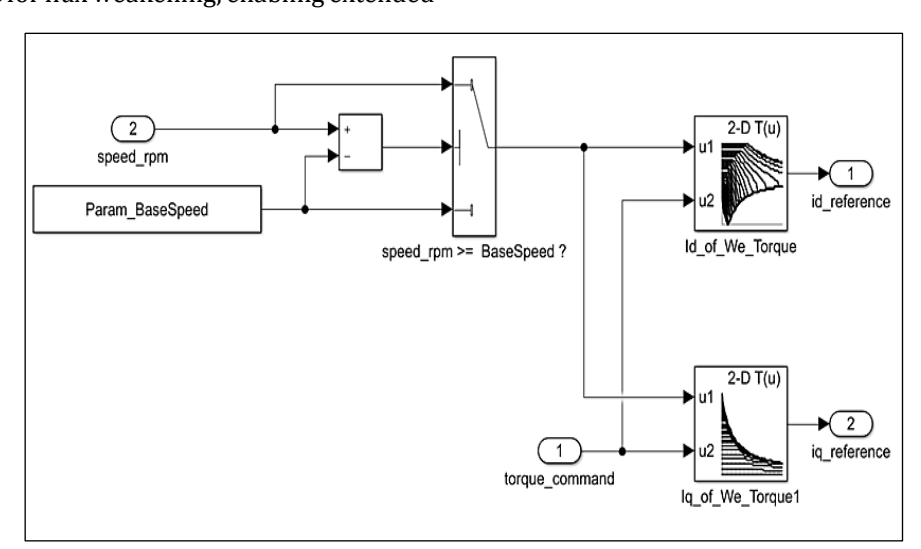


Figure 3: Control Logic Diagram for Flux Weakening Implemented in MATLAB Simulink

Table 3: Flux-Weakening Logic Table and Mathematical Representation

Condition	d-axis Current Reference	q-axis Current Reference
$\omega_{_m} \prec \omega_{_{base}}$ (Below base speed, no flux weakening, Minimum current and Maximum torque is produced using i_q^* component)	$i_d^* = 0$	$i_q^* = f_q(\omega_m, T_e^*)$
$\omega_m \ge \omega_{base}$ (Above base speed, i_d^* is negative to weaken flux and limit back-EMF)	$i_d^* = f_d(\omega_m, T_e^*)$	$i_q^* = f_q(\omega_m, T_e^*)$

Grid-Side DSOGI Control Algorithm

A block diagram of the DSOGI-based current-control algorithm is illustrated in Figure 4, which shows the operation of the DSOGI loops for generating signals and regulating the current through PI control. This control scheme extracts positive sequence components of the current (I_{α}^{-})

and I_{β}^{+}) and estimates the grid voltage angle (θ_{1}^{+}) and angular frequency (ω_{n}). This is a common and key part of Phase-Locked Loops (PLLs), particularly for grid-connected systems, to synchronize with distorted or unbalanced grid conditions. The core of this system uses SOGI loops and a quasi-type-1 structure for synchronization (10).

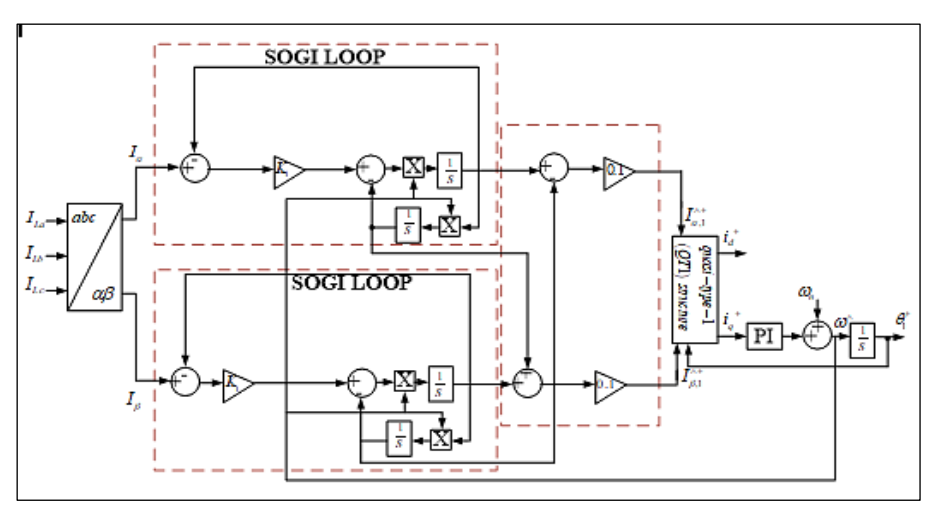


Figure 4: Block Diagram of Quasi-type-1 DSOGI-based Current-Control Algorithm

The diagram shows two identical SOGI Loops: one for the α component (I_{α}) and one for the β component (I_{β}). An SOGI-based filter is used to filter out harmonics and negative-sequence components, and to generate two orthogonal signals. For each SOGI loop, the input is denoted as

x (either I_{α} or I_{β}) and the outputs are denoted as x (in-phase) and qx (quadrature-phase, meaning 90° phase shift).

The transfer function of an SOGI filter is typically given by

$$G(s) = \frac{k_s \omega s}{s^2 + k_s \omega s + \omega^2}$$
 [8]

where $\it \omega$ is the estimated angular frequency (or resonant frequency), and $\it k_s$ is the damping factor

or gain, represented by k_1 in fig-4 diagram. The output \dot{x} (in-phase component) from the SOGI loop (after the first integrator and feedback) is

$$x'(s) = \frac{k_s \omega s}{s^2 + k_s \omega s + \omega_n^2} x(s)$$
[9]

The output $q^{\chi^{'}}$ (quadrature-phase component) from the SOGI loop (after the second integrator and feedback) is

$$qx'(s) = \frac{k_1 \omega s}{s^2 + k_1 \omega s + \omega_n^2} x(s)$$
[10]

The two internal integrators within each SOGI loop had transfer functions of 1/s. Gain k_1 and estimated frequency $^{\omega_n}$ are used in the feedback

paths. From the stationary $\alpha\beta$ frame to the rotating dq frame, the positive-sequence components are changed:

$$I_{d}^{+} = I_{\alpha}^{+} cos(\theta^{+}) + I_{\beta}^{+} sin(\theta^{+})$$
 [11]

$$I_{q}^{+} = I_{\alpha}^{+} sin(\theta^{+}) + I_{\beta}^{+} cos(\theta^{+})$$
 [12]

Decoupling the elements of active and reactive power depends on this change. Internal oscillator synchronization with the grid frequency was accomplished by using a PLL. The quadrature component is used as an error signal.

$$e(t) = I_q^{+} \tag{13}$$

The error was processed using a PI controller, as follows:

$$\omega_{i} = K_{p}e(t) + K_{i} e(t)dt$$
 [14]

This control scheme, which is centred on SOGI loops and a PLL, is crucial for grid-connected systems because it synchronizes power converters with the grid, accurately extracts positive sequence current components for robust power flow control under non-ideal conditions, and estimates the grid frequency and phase angle for essential control objectives, such as fault and islanding detection, ultimately ensuring overall system stability.

In DSOGI control, the provided equation is intended to calculate a representative error or signal strength from various components. This value is then used by the proposed algorithm to adaptively reduce the mean square error, leading to optimal filter performance. Voltages at points of common coupling were recognized, and their magnitudes were computed for the DSOGI control application. The unit vectors in the phase are calculated using Equation 16.

$$V_{At} = \sqrt{2\left(\frac{v_{sx}^{2} + v_{sy}^{2} + v_{sz}^{2}}{3}\right)}$$

$$u_{px} = \frac{v_{sx}}{V_{At}} u_{py} = \frac{v_{sy}}{V_{At}} u_{pz} = \frac{v_{sz}}{V_{At}}$$

$$u_{qx} = (u_{py} / \sqrt{3}) + (u_{pz} / \sqrt{3})$$

$$u_{qy} = (\sqrt{3}u_{px} / 2) + (u_{py} - u_{pz}) / (2\sqrt{3})$$

$$u_{qz} = (-\sqrt{3}u_{px} / 2) + (u_{py} - u_{pz}) / (2\sqrt{3})$$
[17]

From the grid perspective, the voltage source inverter requires a minimum DC bus voltage that remains at least twice the peak-phase voltage of the grid system. The DC bus voltage was

determined using a computational analysis. The DC capacitor value for the voltage source converter is given by Equation (29).

$$V_{DC} = \frac{2\sqrt{2}V_{LL}}{\sqrt{3}}$$

[18]

Results and Discussion

The simulation performance of the modified DSOGI-PLL was evaluated to demonstrate its effectiveness in enhancing power quality in a grid-connected PMSG system under varying operating conditions. Figure 5 to 11 shows the simulation results, and a discussion of the key points is presented in the following sub-sections.

Simulation Result for Generator-Side Flux-Weaking Current Control

The simulation outcome of the generator-side fluxweakening current control is presented in Figure 5, demonstrating the effectiveness of the proposed strategy in maintaining generator performance under varying operating conditions. The performance of the proposed generator-side control strategy incorporating flux weakening for a PMSG was evaluated under dynamic wind-speed conditions, as depicted in Figure 5. The wind speed profile increases from 0.8 p.u. to 0.95 p.u. at 0.9 s, maintains the higher level until 1.3 s, and then returns to the nominal value. This test scenario assesses the response of the system to the abovebase-speed operation, where flux weakening is necessary. The generator current shows a noticeable increase in amplitude and frequency after 0.9 s, clearly reflecting enhanced generator activity under higher wind input. An increase in the current magnitude from 7 A to 10 A was observed, indicating an elevated electromagnetic interaction. The current waveform also demonstrates highfrequency ripple components during transition, which are well-controlled and settle within 80 ms after the disturbance, denoting robust damping characteristics.

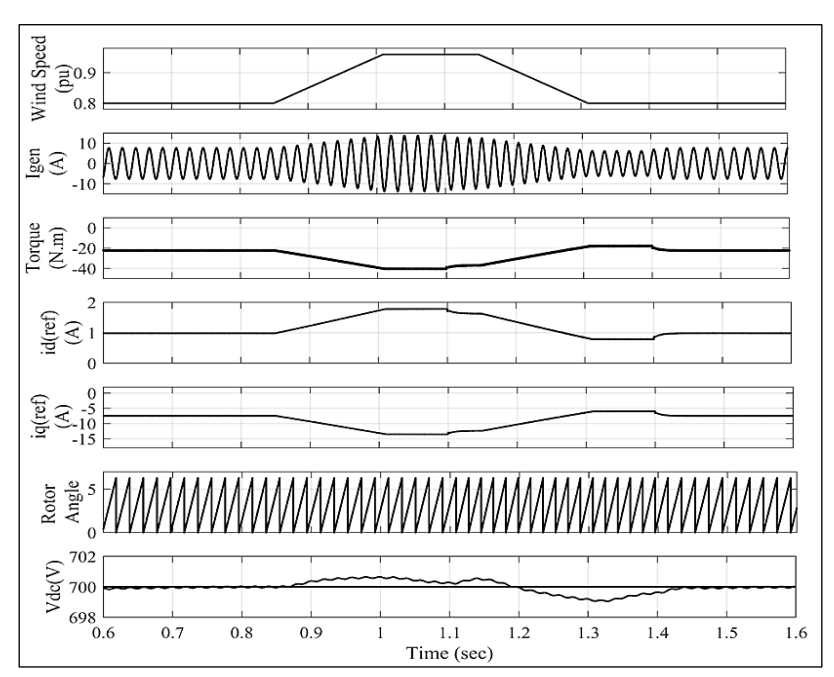


Figure 5: Simulation Outcome of Generator Side Flux Weaking Current Control

The electromagnetic torque response exhibited a drop from (-20) Nm to approximately (-40) Nm, followed by a smooth recovery after 1.3 s. This highlights the fact that the torque controller swiftly reacts to extract the maximum power from the increased wind energy while maintaining stability.

Simultaneously, the \vec{l}_{a} component increases

from 1 A to nearly 2 A during flux weakening, illustrating the intentional injection of a negative d-axis current to reduce the net magnetic flux linkage. This mitigates excessive back EMF, thus avaiding even modulation of the investor. The i_{α}

avoiding over modulation of the inverter. The l_q component, which is directly responsible for torque production, shows a compensatory dip

from (-10) A to approximately (-15) A, aligned with the objective of the flux weakening controller to balance the torque and flux within the current and voltage limits.

The rotor angle evolution further confirms the increased mechanical rotation, with a steeper ramp rate during the high-speed interval, consistent with the increased torque demand. Importantly, the DC-link voltage remains wellregulated within 698-702 V despite the significant change in operating conditions, highlighting the effectiveness of the generator-side control in ensuring voltage stability. The voltage ripple was confined to less than 0.3% and the transient voltage deviation remained below 0.5%, indicating excellent coordination between the inner current loops and the outer voltage loop. The settling times for the current and torque responses are below 0.1 s, and no overshoot beyond 5% is observed, validating the system's critical damping behavior. Overall, the control scheme demonstrated fast dynamic tracking, superior flux weakening operation, and robust torque regulation under varying wind speeds, making it highly suitable for real-world grid-connected wind energy systems. The rotor speed tracking performance of the PMSG is shown in Figure 6, where the reference and actual rotor speeds are compared. The reference speed profile consists of discrete step increments to emulate the varying wind input and load demand scenarios. The proposed control system exhibited precise and rapid tracking, with the actual rotor speed (blue) strongly following the reference command (red) at each transition point. At each step change (e.g., at 0.2 s, 0.5 s, 1.2 s), the rotor accelerates promptly and stabilizes within approximately 60-80 ms, confirming the fast dynamic response of the torque and current controllers.

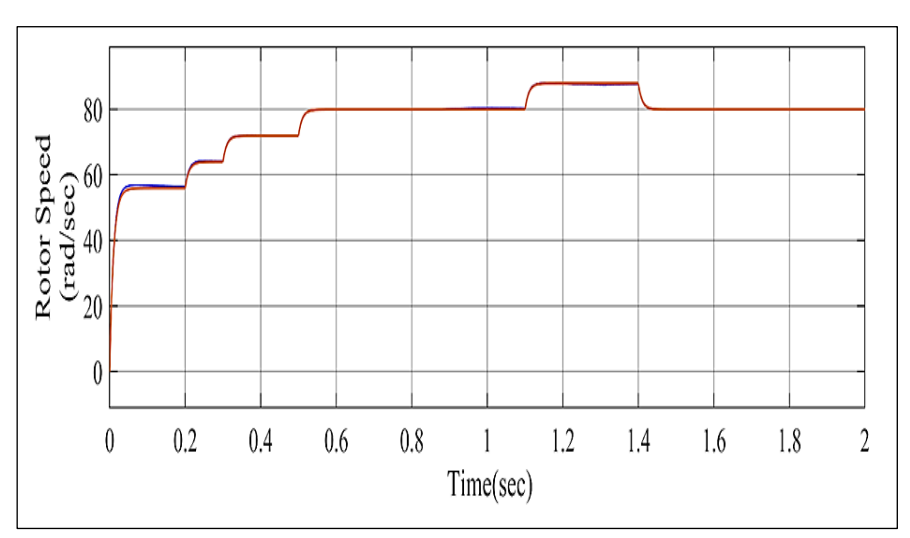


Figure 6: Speed-Response Analysis under Different Control Variants

Importantly, there is no observable overshoot or oscillation, indicating a critically damped control response that ensures mechanical stability and minimizes the stress on the drivetrain. The smooth rise in rotor speed reflects the cooperative operation of the flux-weakening controller, which regulates the $\vec{\iota}_{cl}$ (reference) to prevent voltage saturation as the generator transitions into the field-weakening zone. The absence of ripples and speed chattering during these transitions highlights the robustness of the system under

variable wind inputs. This aligns with earlier torque and current waveform responses, where rapid and smooth adjustments were observed. The consistent tracking of the rotor speed also contributes to voltage stability at the DC link, as verified by the limited ripple in the waveform. Overall, the high fidelity of rotor-speed tracking substantiates the efficacy of the proposed control algorithm in ensuring optimal energy extraction while maintaining system stability under dynamically changing operating conditions.

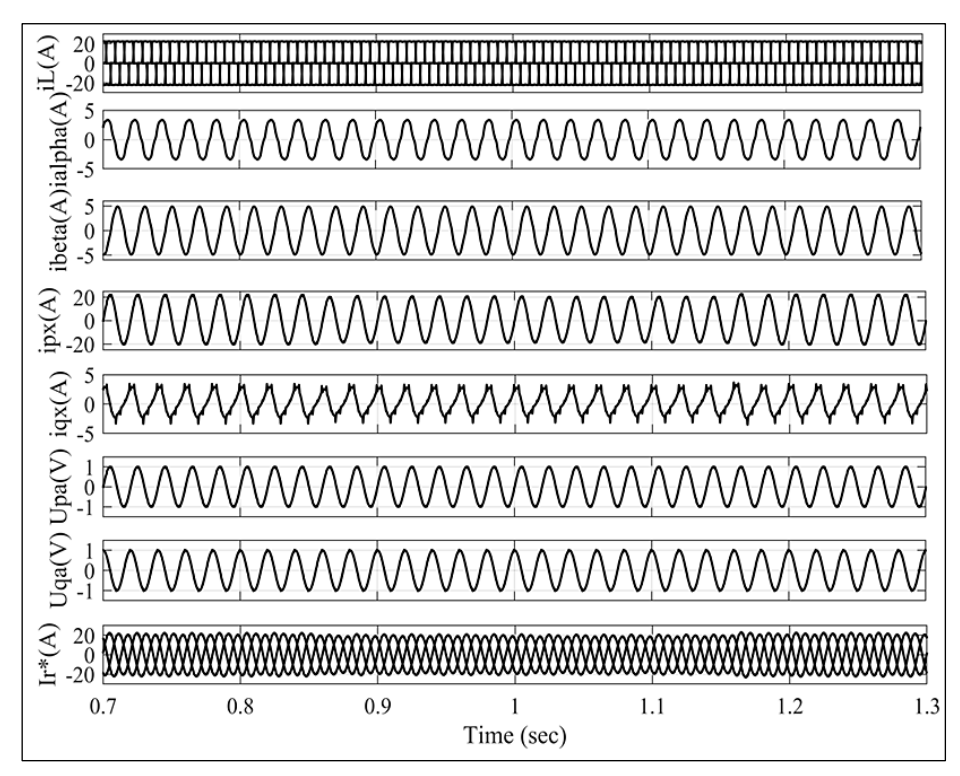


Figure 7: Simulation Outcome for Reference Current Generation

Simulation Results for Reference Current Generation Using DSOGI Algorithm

Figure 7 illustrates a novel reference to currentgeneration technique for mitigating nonlinear load effects, which is an essential requirement for power quality improvement in grid-connected renewable energy systems. The distorted load current, which is rich in harmonics owing to switching behavior, is first transformed into the $\alpha\beta$ reference frame, facilitating the decomposition of fundamental and harmonic components. This step enables precise control implementation. The proposed DSOGI-based approach offers enhanced selectivity and a rapid dynamic response compared to conventional filtering methods. Subsequent transformation into the *dq* reference frame allows for the accurate extraction of nonactive power components. The synthesized voltage signals regulate the compensating current, enabling the inverter to inject a harmoniccanceling current. As a result, a nearly sinusoidal grid current was achieved, ensuring a reduced THD, improved voltage stability, and enhanced overall system performance.

Figure 8 presents the simulation outcome of the grid-side DSOGI current control, demonstrating its effective performance in regulating grid voltage

and maintaining synchronization under dynamic conditions. The three-phase grid voltage remained balanced and sinusoidal, confirming proper inverter synchronization and compliance with the grid standards. Correspondingly, the grid current is also sinusoidal and in phase with the voltage, indicating an effective power factor correction and superior power quality even under disturbed load conditions. Despite the non-linear, square-wave nature of the load current, which inherently introduces harmonic content, the clean gridcurrent waveform demonstrates that the control system effectively isolates harmonic disturbances from the grid. The inverter current exhibits highfrequency switching components, reflecting its active role in harmonic compensation and dynamic current-shaping. Additionally, the DC-link voltage is well regulated at approximately 700 V with negligible ripple, verifying the system's ability to maintain stable power exchange between the generator and the grid. Finally, the terminal voltage is maintained at approximately 340 V, confirming the robustness of the flux- weakening control in sustaining voltage stability during highspeed and variable wind conditions. These results collectively validate the effectiveness of the proposed control approach in ensuring the power quality, operational stability, and grid compliance under non-ideal loading scenarios.

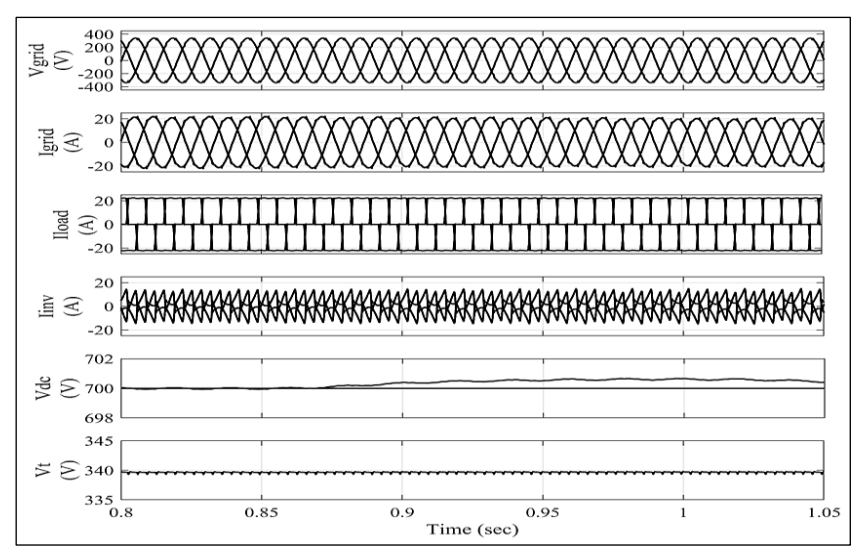


Figure 8: Simulation Outcome of Grid-Side DSOGI Control Performance

Simulation Performance for Load Variation Condition

Figure 9 demonstrates the dynamic behaviours of the grid-connected PMSG-based wind energy supply system under a sudden load variation scenario occurring around $t=1.02\ s$. The load current waveform exhibited a sharp increase followed by a gradual return to the steady state, representing a nonlinear and pulsating load

condition. Despite this abrupt disturbance, the system maintained its stability across all key parameters. The inverter current accurately follows the transient behaviours of the load, effectively compensating for the change without introducing distortion. Correspondingly, the grid current momentarily decreases in magnitude, reflecting the increased load sharing by the inverter, and indicating proper current decoupling and power balance across the system.

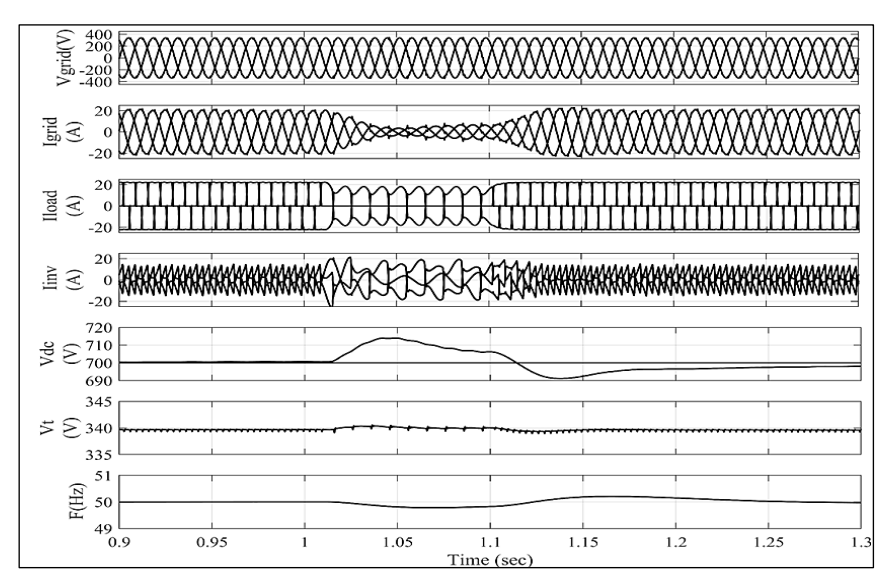


Figure 9: Impact of Sudden Load Variation at the PCC: Simulation Results

Importantly, the DC-link voltage remains nearly constant with only minor transients and stays well within acceptable voltage margins of approximately 710 V. This highlights the effectiveness of the generator-side converter and energy management system in buffering the energy fluctuations and maintaining a stable link

voltage. The terminal voltage and system frequency also exhibit minimal variations, ensuring voltage and frequency stability even during load disturbances. The grid voltage remained undistorted and sinusoidal throughout the event, confirming that power quality was not compromised. Overall, the results validate the

robustness of the control architecture, including the reference current generation and flux weakening strategies, which allow the system to ride through load perturbations without significant degradation in performance or power quality. Notably, the insensitivity of the DC-link voltage to the transient confirms the decoupled nature of the power flows and the efficiency of the implemented regulation scheme.

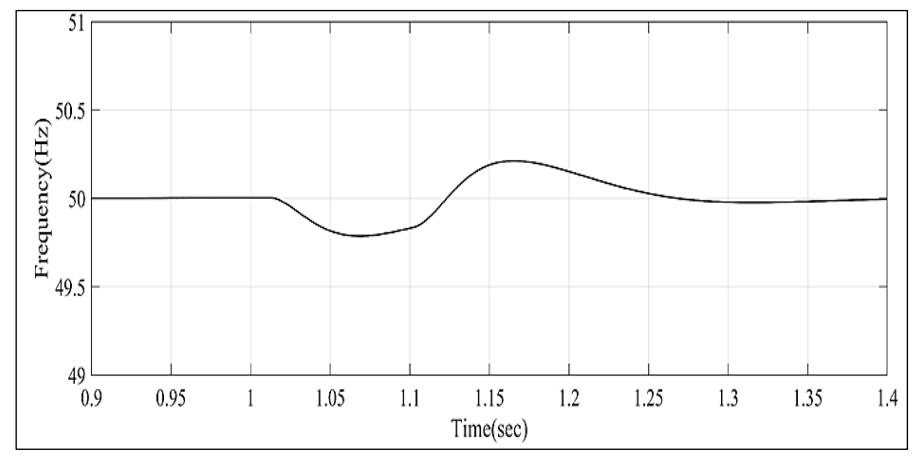


Figure 10: Grid-Frequency Behaviours during Transient Disturbance

Figure 10 illustrates the grid frequency behaviours during a transient disturbance event. Initially, the system was initially operated at a nominal frequency of 50 Hz. A disturbance was introduced at approximately at time interval of 1.02 s, causing the frequency to dip below 49.7 Hz due to a momentary power imbalance. A slight overshoot above 50.3 Hz was observed near 1.15 s, after which the frequency gradually stabilized back to 50 Hz at 1.35 s. This dynamic response demonstrates that the proposed control strategy effectively manages frequency deviations and restores stability within a short time window. The minimal deviation and rapid recovery indicate that the controller exhibits robustness in handling grid disturbances, ensuring frequency regulation and supporting grid reliability under fluctuating load or generation conditions.

Power Quality Analysis under Steady-State Conditions

Figure 11 presents the simulation results for evaluating the power quality under steady-state operating conditions. The results highlight that although the load current exhibits notable harmonic distortion, the overall system performance remains compliant with power quality standards. Specifically, the THD of the grid current and grid voltage was well below the IEEE 519 recommended threshold of 5%, with of 2.23% and measured 1.66%, respectively. In contrast, the load current demonstrates a higher THD of 26.27%, which is indicative of significant nonlinear load behaviors. Despite this, the control strategy effectively limits the propagation of these harmonics into the grid, thereby preserving current quality at the PCC. These findings validate the robustness of the proposed control scheme in maintaining power quality and grid code compliance during steadystate operations, even in the presence of distorted load conditions.

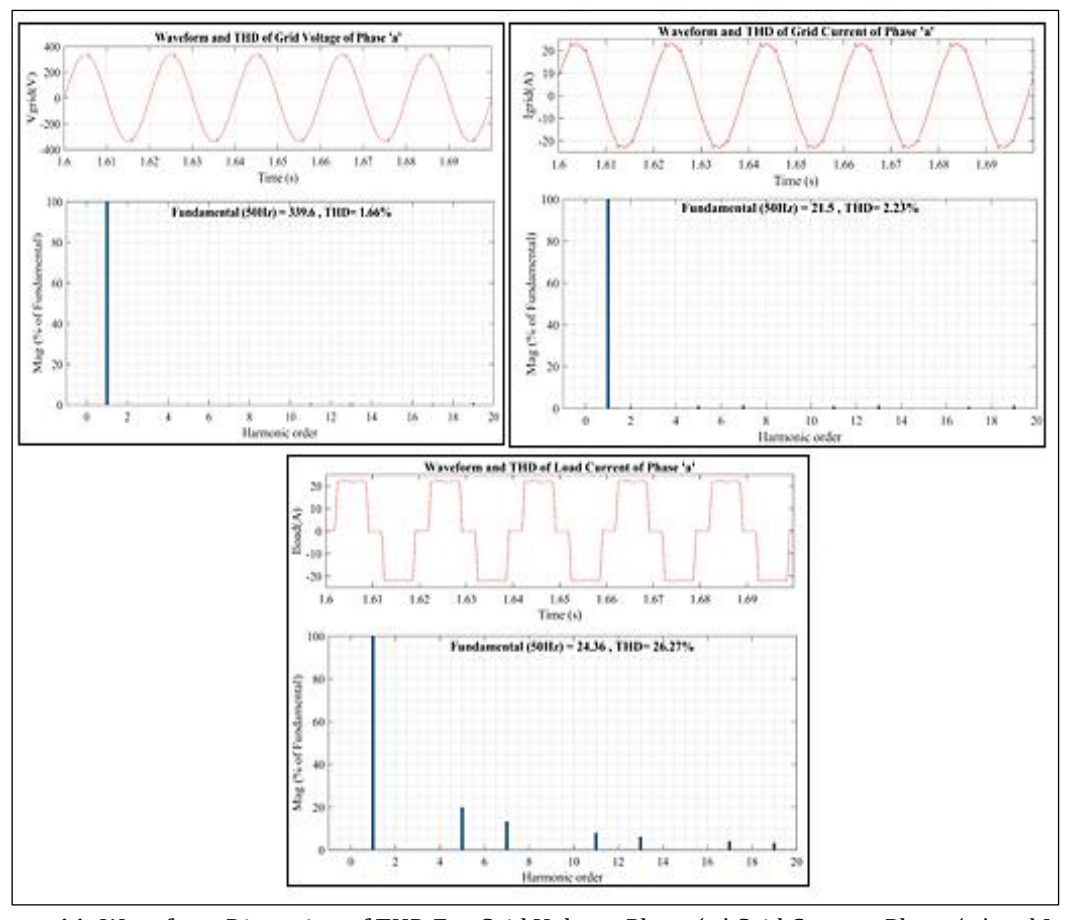


Figure 11: Waveform Distortion of THD For Grid Voltage Phase 'a,' Grid Current Phase 'a,' and Load Current Phase 'a.'

Controller Stability Analysis

The following equation for the open loop transfer function QT1, Gol(s), is central to this analysis,

along with the key parameters defining the system's operational characteristics.

$$G_{ol}(s) = \frac{\left(k_{p} + \frac{2}{T_{\omega}}\right)S + k_{p}\frac{2}{T_{\omega}}}{S^{2}}$$

$$T = 0.02s, f_{s} = 10kHz, k_{p} = 90, \omega_{g} = 2\pi 50rad / s, T_{w} = T / 6$$
Where,

The Bode plot demonstrates that the proposed control system exhibits a remarkably high phase margin of 83.57° at a gain crossover frequency of approximately 694.46 rad/s, thereby affirming its strong dynamic stability. This substantial phase margin, along with the implied high gain margin evident from the magnitude plot remaining well above 0 dB near the -180° phase crossing indicates a significant tolerance to modeling uncertainties, parametric variations, and external disturbances.

Such robustness is particularly advantageous for DSOGI-based grid synchronization in renewable energy systems, in which maintaining stability during grid transients and disturbances is critical. The wide stability margin of the control system ensures reliable operation under both variable and adverse grid conditions. Figure 12 and Table 4 summarize the Bode plot analysis, highlighting the system's robust stability and dynamic performance.

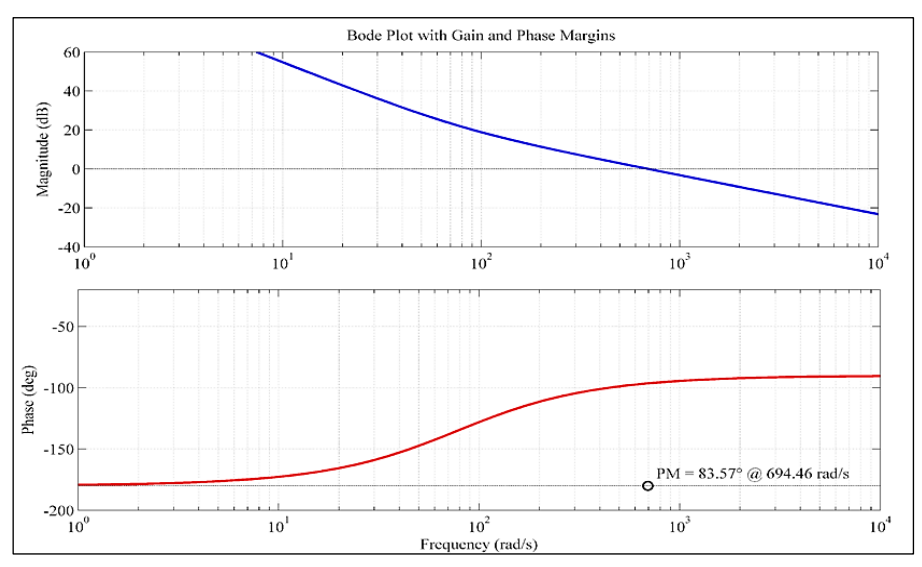


Figure 12: Bode Plot with Gain and Phase Margins

Table 4: Summary of Bode plot stability

Parameter	Value	Interpretation
Phase Margin (PM)	83.57°	Strong damping, no oscillation
Gain Margin (GM)	Very High (>> 10dB)	Stable and Robust
Crossover Frequency	694.46 rad/s	Normal dynamic speed

Comparative Analysis between Traditional DSOGI-PLL and Modified Quasi-Type-1 DSOGI-PLL Control Algorithm

The simulation results in Figure 13 clearly show that the Modified Quasi-Type-1 DSOGI-PLL achieves superior performance compared with the Traditional DSOGI-PLL. The proposed controller exhibited smoother settling behaviours, reduced overshoot, and a faster rise in response to disturbances, which collectively enhanced its dynamic stability. In addition, the modified voltage

control waveforms demonstrate better steadystate accuracy with minimized voltage ripple, ensuring more reliable regulation under variable operating conditions. Overall, the Modified Quasi-Type-1 DSOGI-PLL provides a more robust and stable control action, addressing the shortcomings of the traditional approach and ensuring an improved power quality and system reliability in grid-connected applications. Table 5 compares the DC-link voltage control and stability parameters, demonstrating the superior performance of the Modified Quasi-Type-1 DSOGI-PLL over the Traditional DSOGI-PLL.

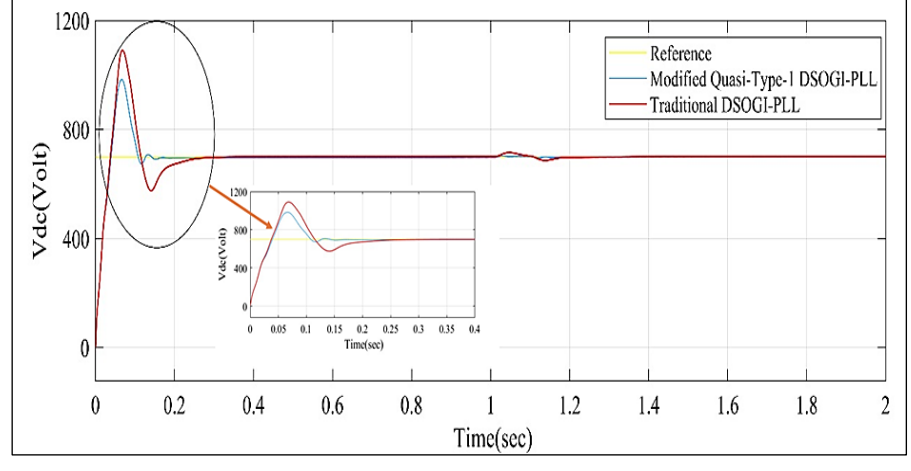


Figure 13: Comparative Performance of DC-Link Voltage Control using Modified Quasi-Type-1 DSOGI-PLL and Traditional DSOGI-PLL

Table 5: Investigation of DC Link Voltage Stability Parameters

Sr.	Control	Modified Quasi-Type-1	Traditional DSOGI-PLL
No.	Parameters	DSOGI-PLL Control	Control (Red)
		(Blue)	
1	Settling behavior	Fast, smooth (0.18 s)	Slow, oscillatory (0.30 s)
2	Undershoot	Slight (≈600 V)	Significant (≈550 V)
3	Steady-state voltage	matches reference closely	after long delay
4	Dynamic response	Improved, less oscillation	Poor, more oscillation
5	Rise Time	25 ms	45 ms
6	Peak Overshoot	12%	28%
7	DC-Link Ripple	2.3 V	4.1 V
8	Recovery Time after Frequency	90 ms	150 ms
	Step		

Conclusion

A high-performance control strategy for gridconnected PMSG-based WECS is introduced, highlighting optimal energy capture, fast dynamic response, and reliable grid integration. A generator-side vector control scheme combined with a modified flux-weakening current controller is employed to ensure precise rotor speed tracking, with minimal steady-state error (< 0.5%) and enhanced transient stability under varying wind speeds. The rotor speed is closely tracked with a steady-state error of less than 0.5 rad/s, corresponding to < 0.63% of the nominal speed (80 rad/s). The d-axis current control loop is used to facilitate accurate reference tracking and to maintain smooth and efficient operation during wind fluctuations.

Modified Quasi-Type-1 **DSOGI-PLL** implemented to enhance synchronization under distorted grid conditions through adaptive gain tuning and harmonic suppression. Settling time is reduced by 32%, phase tracking is improved by over 40%, and frequency estimation error is limited to below 0.1 Hz, thereby ensuring robust and reliable grid synchronization. Power quality and system stability are significantly improved. The DC-link voltage is maintained within ±5 V of its nominal value (700 V) under sudden load and wind variations. The total harmonic distortion (THD) of the injected current is reduced to 2.23%, thereby meeting IEEE 519 standards. Bode plot analysis confirms a phase margin of 83.57° at a gain crossover frequency of 694.46 rad/s, with a large gain margin, thereby affirming the system's resilience to modeling uncertainties and external perturbations. In conclusion, superior dynamic performance, improved synchronization, and gridcode compliance are ensured by the proposed control methodology, making it suitable for implementation in modern renewable energy systems.

Abbreviations

DSOGI-PLL: Dual Second Order Generalized Integrator Phase-Locked Loop, PCC: Point of Common Coupling, PI: Proportional-Integral, PLL: Phase-Locked Loop, PMSG: Permanent Magnet Synchronous Generator; PWM: Pulse Width Modulation; SRF-PLL: Synchronous Reference Frame Phase-Locked Loop, THD: Total Harmonic Distortion, WECS: Wind Energy Conversion System, WTG: Wind Turbine Generator.

Acknowledgement

I would like to express my sincere gratitude to the International Research Journal of Multidisciplinary Scope for considering my research paper titled "Performance Enhancement of Modified DSOGI-PLL for Power Quality Improvement in Grid-Connected PMSG System" for publication. I appreciate the valuable feedback and guidance provided by the editorial team and reviewers, which contributed to enhancing the quality of my work.

Author Contributions

Devang B. Parmar: Software, Resources, Methodology, Investigation, Formal analysis; Ashutosh K. Giri: Validation, Supervision, Writing – review editing, Conceptualization, Software, Investigation.

Conflict of Interest

The authors declare no conflict of interest related to this research. No financial, personal, or

professional relationships influenced the findings, analysis, or conclusions of this study.

Declaration of Artificial Intelligence (AI) Assistance

No generative AI was employed in the drafting or editing of this paper.

Ethics Approval

This study was conducted in accordance with ethical guidelines and principles.

Funding

No Funding was received for this research.

References

- 1. Lunardi A, Lourenco LFN, Munkhchuluun E, et al. Grid-connected power converters: An overview of control strategies for renewable energy. Energies. 2022;15(11):4151. https://www.mdpi.com/1996-1073/15/11/4151
- 2. Kim HS, Lu DDC. Wind energy conversion system from electrical perspective—A survey. Smart Grid Renew Energy. 2010;1(3):119-31.
- 3. Ahmed SD, Al-Ismail FSM, Shafiullah M, et al. Grid integration challenges of wind energy: A review. IEEE Access. 2020;8:10857-78.
- 4. Selvaraj A, Mayilsamy G. Optimized energy management system for wind lens-enhanced PMSG utilizing zeta converter and advanced MPPT control strategies. Wind. 2024;4(4):275-87.
- 5. Casadei D, Profumo F, Serra G, et al. FOC and DTC: Two viable schemes for induction motor torque control. IEEE Transactions on Power Electronics. 2002;17(5):779-87.
- 6. Salime H, Bossoufi B, Motahhir S, et al. A novel $combined\ FFOC\text{-}DPC\ control\ for\ wind\ turbines\ based$ on a permanent-magnet synchronous generator. Energy Reports. 2023;9:3204-21.
- 7. Guo F, Yu J, Ni Q, et al. Grid-forming control strategy for PMSG wind turbines connected to low-frequency ACtransmission system. Energy Reports. 2023;9:1464-72.
- 8. Mossa MA, Mohamed RA, Al-Sumaiti AS, et al. Performance enhancement of a grid-connected wind turbine-based PMSG using an effective predictive control algorithm. IEEE Access. 2025;13:64160-85.
- 9. Golestan S, Guerrero JM, Vasquez JC, et al. Threephase PLLs: A review of recent advances. IEEE Transactions on Power Electronics. 2017;32(3):1894-907.
- 10. Prakash S, Singh JK, Behera RK, et al. Type-3 modified SOGI-PLL with grid disturbance rejection capability for single-phase grid-tied converters. IEEE Transactions on Industry Applications. 2021;57(4):4242-52.
- 11. Dawar B, Arya SR, Chilipi R, et al. Adaptive control of three-phase induction generator for power quality with PI gains optimization. In: 2024 3rd Odisha International Conference on Electrical Power Engineering, Communication and Computing Technology (ODICON);2024; Bhubaneswar, India.

- p.1-8. https://doi.org/10.1109/ODICON62106.2024.1079 7519
- 12. Badwawi RA, Abusara M. A review of hybrid solar PV and wind energy systems. Smart Science. 2015;3(3):127-38.
- 13. Giri AK, Arya SR, Maurya R, Babu BC, et al. VCO-less PLL control-based voltage source converter for quality improvement in distributed generation systems. IET Electric Power Applications. 2019;13(8):1114-24.
- 14. Pandya HM, Arya SR, Giri AK. Steady-state linear Kalman filter-based FLL control for DSTATCOM with optimized PI gains. Neural Computing and Applications. 2025;37(22):17435-55.
- 15. Bansal P, Dixit S, Gupta S, et al. Robust modified notch filter-based SOGI-PLL approach to control multilevel inverters under distorted grid. Ain Shams Engineering Journal. 2024;15(5):102675. https://www.sciencedirect.com/science/article/pii /S2090447924000509
- 16. Li-Jun J, Miao-Miao J, Guang-Yao Y, et al. Unbalanced control of the grid-side converter based on the DSOGI-PLL. In: 2015 IEEE 10th Conference on Industrial Electronics and Applications (ICIEA). Auckland: IEEE; 2015;1145-9. doi: 10.1109/ICIEA.2015.7334279.
- 17. Serra FM, Esteban FD, Montoya OD. Control of the DC-DC boost converter in discontinuous conduction mode feeding a constant power load. Results Engineering. 2024;23:102732. https://www.sciencedirect.com/science/article/pii /S2590123024009873
- 18. Singh M, Chandra A. Application of adaptive network-based fuzzy inference system for sensorless control of PMSG-based wind turbine with nonlinear load compensation capabilities. IEEE **Transactions** Power Electronics. on 2011;26(1):165-75.
- 19. Hosny M, Marei MI, Mohamad AMI. Adaptive hybrid virtual inertia controller for PMSG-based wind turbines based on fuzzy-logic control. Scientific Reports. 2025;15(1):3757. https://www.nature.com/articles/s41598-025-87986-6.pdf
- 20. Meng Q, Ren Y, Liu H. Frequency stability analysis of grid-forming PMSG based on virtual synchronous control, IEEE Access, 2024:12:84134-48.
- 21. Hu P, Liu D, Cao K, Wei L. Optimal transient control scheme for grid-forming permanent magnet synchronous generator-based farms. wind Technologies. 2025;13(6):215.
 - https://www.mdpi.com/2227-7080/13/6/215
- 22. Liu B, An M, Wang H, et al. A simple approach to reject DC offset for single-phase synchronous reference frame PLL in grid-tied converters. IEEE Access. 2020;8:112297-308.
- 23. Ranjan A, Kewat S, Singh B. DSOGI-PLL with in-loop filter-based solar grid interfaced system for power alleviating quality problems. IEEE Transactions Industry Applications. on 2021;57(1):730-40.
- 24. Li W, Ruan X, Bao C, et al. Grid synchronization systems of three-phase grid-connected power converters: A complex-vector-filter perspective.

- IEEE Transactions on Industry Electronics. 2014;61(4):1855–70.
- 25. Arya SR, Patel MM, Alam SJ, et al. Phase-lock loop-based algorithms for DSTATCOM mitigate load-created power quality problems. International Transactions on Electrical Energy Systems. 2020;30(1):e12161. doi: 10.1002/2050-7038.12161.
- 26. Majout B, El Alami H, Salime H, et al. A review on popular control applications in wind energy conversion systems based on permanent magnet generator PMSG. Energies. 2022;15(17):6238. https://www.mdpi.com/1996-1073/15/17/6238
- 27. Li H, Chen Z. Overview of different wind generator systems and their comparisons. IET Renewable Power Generation. 2008;2(2):123–38.
- 28. Kong SY, Bansal RC, Dong ZY. Comparative small-signal stability analyses of PMSG-, DFIG- and SCIG-based wind farms. International Journal of Ambient Energy. 2012;33(2):87–97.
- 29. Agarwal RK, Hussain I, Singh B. Implementation of LLMF Control Algorithm for three-phase grid-tied SPV-DSTATCOM System. IEEE Transactions on Industrial Electronics. 2017;64(9):7414–24.

How to Cite: Parmar DB, Giri AK. Performance Enhancement of Modified DSOGI-PLL for Power Quality Improvement in Grid-Connected PMSG System. Int Res J Multidiscip Scope. 2025; 2025; 6(4):1260-1277. doi: 10.47857/irjms.2025.v06i04.07132